

VERY HIGH RESOLUTION FUNCTIONAL BRAIN MAPPING

Justification of Resources Requested

During calendar 2015 we anticipate acquiring a minimum of 70 40-minute MEG recording sessions. With a processing requirement of ≈ 150 cpuHours per second, this represents a need for a minimum of 25,000,000 cpuHours on the Open Science Grid. These studies will be obtained from neurologically normal volunteers, patient volunteers with chronic sequelae of traumatic brain injury, and patient volunteers with positive HIV sero-status.

This renewal includes a request for continued access to Blacklight and the PSC Data SuperCell. These are used to aid in job management, data flow, and backup for both results and software.

Special Request¹: Our group has been funded by the Department of Defense to develop and evaluate a comprehensive patient-centered approach to clinical management of head injury in veterans and active duty military personnel. Each patient volunteer will be thoroughly evaluated by a team of physicians and neuropsychologists using anatomic and functional measures including both a standard and an individually tailored neuropsychological battery, MR brain imaging, MR spectroscopy, white matter tractography, PET, and magnetoencephalography (MEG) functional brain imaging. This testing will be obtained over a 36 hour period at the end of which the team will meet to decide on treatment recommendations. There is a 30 hour window during which the processing and analysis of the MEG recordings must be completed in order to be available for the deliberations at an adjudication meeting.

To accomplish this within the time constraints, we request dedicated access to 15,000 cores continuously for one 24 hours approximately every two weeks. We will be able to provide precise scheduling information well in advance of each study. The jobs will utilize the fully HIPAA compliant code which is used for all of our jobs.

This is not a request for a guarantee. If the full requirement is not met, the value of the effort is not negated. Rather the reliability of the results will be reduced but the work is organized to obtain useable results from partial completion of the total job requirement.

The critical period for doing the calculation will begin at about 6 PM EST Tuesday night. We anticipate a total of 50 such studies beginning in November, 2014 and extending over the next 2 years. Our request therefore is for $\approx 15\%$ of the current grid capacity for one 24 hour period out of each 2 weeks on a well-defined schedule.

For each 24 hour period, once the work has begun we will be able to provide an estimate of when the work will complete. This will allow the XSede and OSG operations staff to schedule resetting the priorities and other system settings to their normal operational

¹ This request will also be presented to the OSG Governing Council at their meeting in late October, 2014.

values. On the other hand we will make sure that there is sufficient work queued to fully utilize whatever cycles are provided to insure that there is no waste.

Acknowledgements

We gratefully acknowledge the ongoing assistance of the OSG staff. Their efforts on our behalf have been invaluable. We particularly wish to thank Mats Rynge, Marko Slyz, Scott Teige, Rob Quick, and Chander Sehgal.

Introduction

Concussion is an important clinical entity effecting millions of people each year in the US alone. Whereas $\approx 80\%$ fully recover within three weeks, many suffer with persistent problems for months or years which markedly effect their quality of life. In spite of its prevalence, concussion is so poorly understood that the primary means by which a diagnosis is obtained is by history.

Both computed tomography (CT) and magnetic resonance brain imaging (MRI) provide millimeter (mm) resolution for structural images of bone, blood and other fluids, white and grey brain matter, and surrounding soft tissues within the head. Diffusion tensor MRI and more recently developed variants including High Definition Fiber Tractography (Verstynen et al., 2011) provide visualization of the trajectories of white brain matter tracts with 2.5 mm resolution. Yet imaging findings are present in less than 20% of those who present to a hospital emergency room. Almost nothing is known regarding the mechanism of loss of consciousness, the signature event which defined concussion for decades. Very little is known regarding how to predict the long term sequelae of concussion or what to do to treat it.

Behavioral measures of attention, memory, decision making, etc. are sensitive to concussion but not specific. The hope is that measures of brain function specific to concussion might be found which correspond to these behavioral measures and that that might lead to better understanding and treatment. But to date functional brain measures (Table 1) have provided only weak discriminators of differences between pathological and normal groups, offering little hope that they will prove useful for individual diagnosis and treatment or provide insight into mechanism. Here are recent reviews of findings in concussion using functional brain imaging: fMRI² (Shenton et al, 2012; Rosenbaum and Lipton, 2012; McDonald et al, 2012; Slobunov et al, 2012; Lin et al, 2012; Dziemianowicz et al, 2012; Gardner et al, 2012; Keightley et al, 2012; Kutcher et al, 2013; Fox et al, 2013), diffusion tensor imaging³ (Shenton et al, 2012; Slobunov et al, 2012; Gardner et al, 2012; Fox et al, 2013), spontaneous EEG (Davis et al, 2009; Arciniegas, 2011; Kutcher et al, 2013), event related potentials (Davis et al, 2009; Ellemberg et al, 2009; Gosselin et al, 2010), MEG (Davis et al, 2009; Gonzalez and Walker, 2011; Kutcher et al, 2013), and MRS⁴ (Prabhu, 2011; McCullough and Jarvik, 2011; Gonzalez and Walker, 2011; Choe et al, 2012; Slobunov et al, 2012; Lin et al, 2012).

The work proposed here is based on an innovative advance in Magnetoencephalographic (MEG) functional brain imaging. It builds on the capabilities of existing MEG technology e.g. Hamalainen & Ilmoniemi, 1994; Krieger, 1995; Tormenti et al., 2012, to produce improved spatial resolution while solving problems which have

² Functional magnetic resonance imaging.

³ DTI produces images of the fibers which connect neural populations. A more powerful follow on method, high definition fiber tractography, can be fused with MEG virtual recording (MVR) to produce analysis of network dynamics and interactions at much higher resolution than previously achieved.

⁴ Magnetic resonance spectroscopy.

markedly limited the utility of MEG till now. In particular, it produces high confidence estimates for all of the following:

1. the number of active MEG sources at each moment,
2. the spatial extent of the coordinated neural activity which comprises a source,
3. the location of each source,
4. the time course of the neuroelectric current flow at each of the identified source locations.

The established capabilities of MEG along with these new ones enable very high resolution noninvasive recording of the neuroelectric currents within the brain as if from 2,000,000+ directly implanted electrodes, hence the name of the method, MEG Virtual Recording (MVR).

Sensitivity	Examples	Resolution	
		Spatial ⁵	Temporal
calcium, phosphorous, ¹³ carbon, ...	MRS ⁶	1 cm	10 min
Regional blood flow or receptor specific neuroactive molecules	SPECT ⁷	1 cm	10 min
blood flow and/or blood oxygenation	NIRS ⁸	1 cm	50 msec
	PET ⁹	1 cm	10 min
	fMRI ¹⁰	2 mm	50 msec
neuroelectricity	EEG ¹¹	2 cm	1 msec
	MEG ¹²	2 mm – 2 cm	1 ¹³ msec

Table 1: Functional Imaging Modalities

⁵ This is an estimate for the linear dimension of a volume over which the functional measure is confined.

⁶ Magnetic resonance spectroscopy: MRS provides a single “snapshot” spectrogram from which the concentration of a compound with the excited volume may be estimated. These may be used to draw inferences about energy metabolism, etc. The cited spatial resolution of 1 cm is obtainable with a 7T magnet.

⁷ Single photon emission computed tomography (SPECT): This method provides a single “snapshot” of the distribution of a radioactively labeled compound.

⁸ Near infrared spectroscopy (NIRS): This method is sensitive to perfusion and/or oxygenation of the cortex near the surface of the brain adjacent to the skull. The time resolution cited, 50 msec, is the nominal sampling rate. Tissue perfusion/oxygenation changes relatively slowly with peak change several seconds following a stimulus.

⁹ Positron emission tomography (PET)

¹⁰ Functional magnetic resonance imaging (fMRI): The time resolution cited, 50 msec, is the sampling rate at which image slices are routinely obtained. Tissue oxygenation changes relatively slowly with peak change at 4-6 seconds following a stimulus. 2 mm is a typical linear dimension for an fMRI voxel. The common strategy of requiring statistical significance in 10 or more adjacent voxels may erode the useable resolution to 5 mm voxels.

¹¹ Electroencephalography (EEG): Electrophysiological waveforms evoked by either auditory or somatosensory stimuli are readily obtained with time resolution of 0.1 msec resolution. The known sources for this very short latency neuroelectric activity are in the brainstem, midbrain and thalamus. But the more widely utilized cortical waveforms, although recordable at high sampling rates, have a slower time course with detectable changes occurring over several msec. This latter is also true for MEG recordings.

¹² Magnetoencephalography (MEG): MEG is relatively insensitive to neuroelectric activity originating in the brainstem, midbrain, and thalamus. The 2 mm spatial resolution cited in the table is achieved by standard MEG methods under optimal conditions utilizing averaged sensory evoked responses. It is also achieved by MVR (reported below) using raw single trial data. For averaged evoked responses outside primary sensory areas, spatial resolution achieved by standard MEG methods is eroded to 1 cm or more.

¹³ MEG recordings are typically sampled at 1 KHz with anti-aliasing filtering with knee at 330 Hz.

The functional brain imaging information provided by the MVR search is multiplied many fold compared with other current functional brain imaging methods, both because MVR produces estimates with high confidence and resolution for many simultaneously active sources within the brain, and because it does so for every time epoch as second after second of raw data is streamed through the method's processing pipeline. This is in contrast to methods which produce low resolution or single source measures from data which has been collapsed using signal averaging. This fact holds out the hope that extant data which has previously been analyzed with such methods may yield more comprehensive information if processed using the MVR search. The improved sensitivity and spatiotemporal specificity of MVR may also demonstrate previously undetectable differences in brain activation due to experimental or pathologic differences in behavioral function.

The MVR search is a transformational functional brain imaging technology. It provides estimates of local brain tissue activation with spatiotemporal resolution at least 2 order of magnitude better than previously achievable. When fused with High Definition Fiber Tractography, it enables identification of the sequence and timing of activation used by the brain to perform a task. The raw data handling and activation sequencing capabilities of MVR enable tracking of seizure propagation and identification of seizure sources by back tracking.

MVR is broadly applicable. Several teams of clinician researchers and neuroscientists are committed to using the method in their work. Several of these collaborations are reflected in the list of grants.

Research Justification

The heterogeneity of head injury is well known. Even the gross and readily visualized injuries which produce moderate and severe TBI have great variety. It seems likely that when visualized and understood, the more mild injuries will show even greater variability.

Positive imaging findings (CT and MRI) are present in less than 20% of concussions. High definition fiber tractography enables visualization of broken neural fibers with much high resolution and accuracy than previously obtainable. This new imaging method will likely produce positive findings in a significant fraction of concussions which show no abnormalities on CT or MRI. But it is likely that there will remain a large population of concussion patients without fiber tract disruption.

The search for differences between normal and pathological groups is potentially sensitive only to those pathological changes which the members of the group have in common. But for progressively milder injuries, if the heterogeneity increases, then the individual differences will dominate more, reducing our ability to identify discriminators. While the clinical imperative is to obtain reliable and meaningful measures from a single individual, here we have an additional charge to do so in order to achieve our related research objectives. For as the differences between individuals outstrip the group differences with progressively milder injuries, we must find ways to understand normal

and pathological processes in each individual to advance our understanding and ability to manage these injuries. This is not a novel argument but is likely particularly relevant in the study of concussion given the lack of success of the massive ongoing efforts to understand it. The likely validity of the argument supports the longitudinal emphasis in our work, i.e. obtaining repeat studies many months apart from the same individuals to enable identification of changes within the individual.

The primary cause in head injury to which brain pathology has been attributed is mechanical shock. This is the impetus for the search for pathological changes in structural brain images. But it is plausible that pathological changes are also mediated by over driven neuronal activity originating in the brainstem caused by transient high intensity input at the moment of impact. Particularly the upward propagating effects of paroxysmal outflow from the brainstem would likely depend on the current state of the receiving supra tentorial structures, adding to variability in pathologic function seen with concussion.

The transient hyper maximal stimulation at the moment of concussion typically includes loud sound (cochlear nerve), intense pressure and pain (trigeminal nerve), and large head movements (vestibular nerve). The resulting outflow could include the vagus nerve, resulting in transient asystole with resultant hypotension and loss of consciousness. It could also include upward projecting pathways, activating the basal ganglia, hypothalamus, thalamus, and other supra tentorial structures.

This upward going abnormal wave of activation could potentially induce persistent changes in the excitability of widely distributed neural populations throughout the brain. While these putative changes likely would fall within the range of normal, the consequent alterations in the patterns of excitation which carry information could be sufficient to produce alterations in timing, slower or faster, and/or errors in information transmission, resulting in the disruptions in cognitive function seen in behavioral testing. The idea is that the resultant new patterns, being normal but new, must be learned. Just as transient degradation in physical coordination is seen in children undergoing a growth spurt, concussion may produce loss of coordination degrading information transmission and cognitive function which progressively resolves with learning.

Measures with sufficient temporal and spatial resolution to explore these ideas have not been available till now. This includes MEG measures which have been relatively static for decades. The discovery of referee consensus optimization and its application to MEG recordings has changed that. With this new method the sheer quantity of reliable information extracted from MEG recordings is conservatively 1000 times more than that previously obtainable. Fusion with high definition fiber tractography will enable full use of that neurophysiological information to produce dynamic high resolution functional imaging of the brain processes which underlie the behavioral changes seen in concussion.

The recent findings detailed below support the ambitious direction of our work. We have found strong evidence using a well controlled over learned task that the task-

relevant activity of a functional brain unit is measurable with mm resolution and that the distance scale over which a neural population cooperates as a functional unit is ≈ 3 mm with 6 mm as the upper limit.

The measurement of “scale” is a critical step in understanding how brain activity mediates task performance. That in turn is central to our approach to understanding the brain mechanisms which underlie the disruption of cognitive processes characteristic of concussion and the natural history of recovery. Knowing both the spatial and temporal scale of task relevant brain mechanisms enables targeting measurement modalities which have the potential to provide images of the pathology present in concussion. Note that for time scale, we need only look to behavioral results to see that measurements with less than 100 msec latency are needed, e.g. Figure 3. The event related potential literature supports the need for measurements with less than 10 msec latency.

Research Objectives and Recent Findings

Our research objectives are to elucidate the nature and localization of both normal and abnormal brain mechanisms which mediate task performance. The accompanying clinical objective is to identify both sensitive and specific functional brain imaging measures for pathologies for which no such measures currently exist, e.g. concussion, post-traumatic stress disorder (PTSD). The hope is that these measures will prove useful in understanding the causal mechanisms for these pathologies and consequently in enabling discovery of treatments and/or cures.

Our initial measurement goal is to identify which brain areas are activated during the course of task performance and when are they activated.

1. How large are those areas, i.e. what is the distance scale over which neurons cooperate to produce measurably unified activity? This distance scale is arguably the size of a functional unit if the measurable activity can be related to the task. The results of our work on the grid detailed below suggest that this distance scale is 2-3 mm and we therefore term these populations: “functional units.”
2. What is the time course of that activity? How long does it persist? When does the cooperative activity begin and when does it end?
3. Are there characterizable relationships between the activities of identified functional units? Any such relationships are presumed to be mediated by fiber connections between the units. In many brain areas at this distance scale, the connections may be visualized by High Definition Fiber Tractography (Verstynen, 2011) and the time course of the activities measured by MVR may be fused with the localization to study the dynamics of the network of functional units. Are there candidate mechanisms by which those dynamics can be disrupted which could be caused by concussion?
4. What can be inferred regarding the mechanisms by which the cooperative activity with functional units occurs and what its function¹⁴ is? Are there candidate

¹⁴ A useful working concept is that each unit’s function is recognition of the pattern of excitatory input it receives, producing (1) fusion of the patterns present in the inputs from multiple functional units and

mechanisms by which cooperativity can be disrupted which could be caused by concussion?

The resolving power of MVR. The results obtained during the tenure of the current (2013) XSede grid allocation period provide evidence for 2-3 mm with 6 mm as the upper limit as the distance scale over which neural populations cooperate to form a functional unit (Figures 1,4,5,6,7). These results are reviewed below.

As currently implemented, MEG Virtual Recording (MVR) is applied to a single 80 msec raw single trial data epoch at a time. Each source which is accepted by the method is characterized by a supra-threshold value for the referee consensus cost function, 3 location coordinates, a normalized 80 point waveform, and 2 amplitude values which when multiplied by the waveform, produce the amplitudes of two orthogonal components

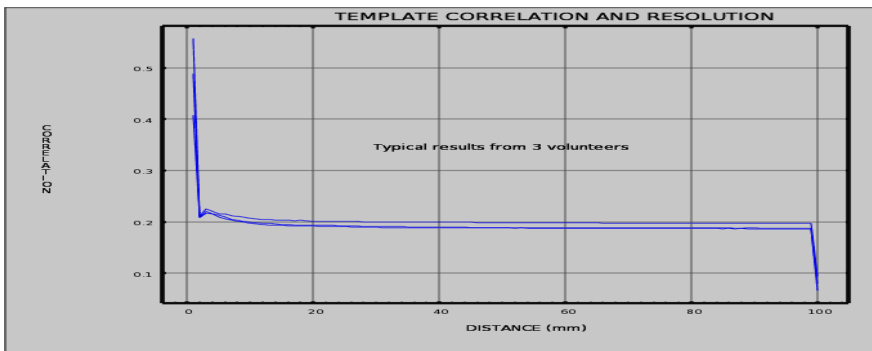


Figure 1. The correlation between all pairs of coincident source templates is shown as a function of distance between the sources from 1 mm to 100 mm. The absolute value of the correlation was used in each case. The variance in the measure was 0.02. These results demonstrate resolving power of 1-2 mm. The results shown (3 subjects) were typical.

of the time course of the current source. As currently implemented, at most one source may be found for each 80 msec time epoch within each of the ≈ 3000 8mm^3 voxels which cover the brain.

For each 80 msec data epoch for all volunteers, 500-1500 sources were accepted. Note that the threshold for acceptance has a nominal p-value $< 10^{-12}$. While the number of sources is higher than expected, it is plausible that this accurately represents the number of sources within the brain which are simultaneously active at any one moment. In fact given the limitations of the method, it is likely that the true number of simultaneously active sources is higher.

All standard MEG methods produce estimates of the time course of source activity with spatial resolution of 1 cm or more. This is so even for the gold standard Equivalent Dipole Source localization which can ideally produce estimates of the location of a source with near mm resolution. We obtained measures of the resolution of MVR time

enhancement of both (2) the spatial contrast of the fused patterns and (3) the synchrony of its output activity for transmission (Freeman and DiPrisco, 1986; Krieger, 1995{2}).

course estimates by computing the average correlation between simultaneously active sources and plotted these as a function of distance between the sources.

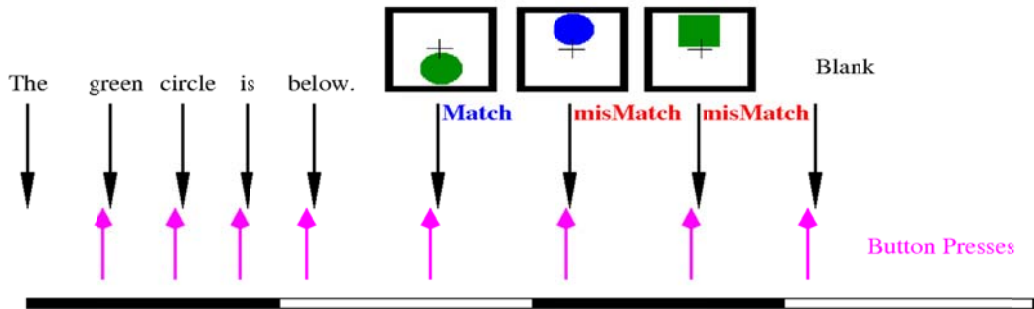


Figure 2. MEG recordings were obtained from normal and concussed volunteers while they performed the repetitive (320 trials) task schematized above. The bar at the bottom is 4 sec long. The black arrows indicate separate stimuli. The magenta arrows indicate responses to the preceding stimulus. The 2nd-5th word stimuli were triggered by a button press with the index finger. If the test figure matched the sentence, the response was a button press with the index finger. If not, the response was a button press with the middle finger.

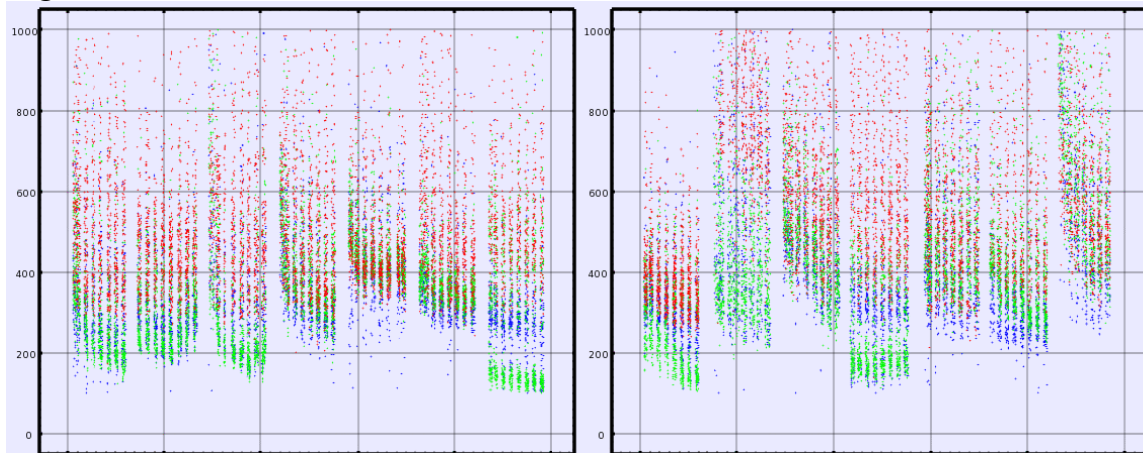


Figure 3. Response times (msec) are plotted on the vertical axis for word stimuli (blue: the, is; green: color, shape, place) and test figure responses (red). Each narrow column represents a 40 trial block. Each group of 8 columns represents the sequence of 40 trial blocks for a single volunteer, 7 normals (left panel) and 7 concussed with persistent symptoms (right panel).

Results for 3 volunteers are shown in Figure 1. For distances greater than 1 mm, the average correlation is nearly flat and is close to 0.2. For random variables a correlation of 0.2 (n=80) has two-tailed p-value = 0.075. But correlations between time series are expected to be inflated due to auto-correlation structure within each series. In any case, these correlations are extraordinarily low, considerably lower than would be found in recordings from a low impedance grid placed directly on the brain. This result provides strong evidence that MVR can resolve the activity of intra-cranial sources less than 2 mm apart using raw single trial data.

The size of functional units within the brain. The number of sources accepted by MVR within each voxel was counted. For voxel sizes ranging from 24mm^3 to 2mm^3 , the count for trials which were a match (index finger button press) were compared with the count for trials which were a mismatch (middle finger button press). The χ^2 statistic and

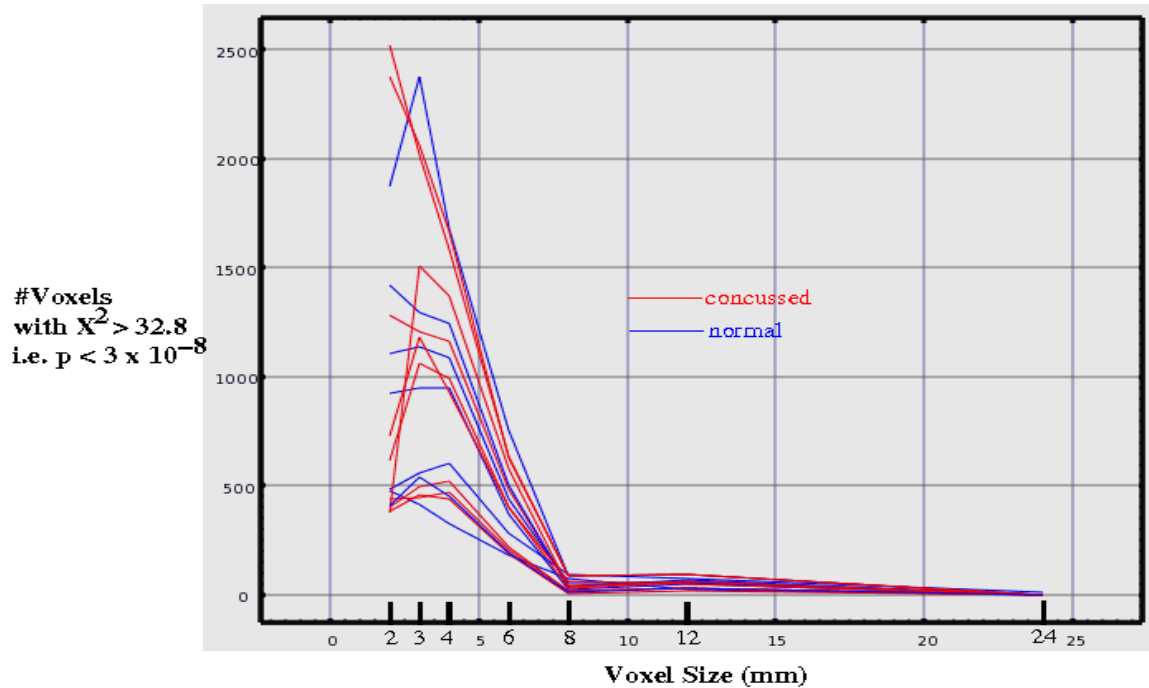


Figure 4. Differential activation results for 15 volunteers are shown. For each, sources were counted from a 560 msec epoch of MEG beginning with button press in response to test figure presentation. The count when the target was a match vs a mismatch was tested for significant difference. The number of voxels for which the corresponding $p < 3 \times 10^{-8}$ ($\chi^2 > 32.8$) is plotted against the size of the voxel, 24/12/8/6/4/3/2 mm. The corresponding total #voxels \approx 100/1000/3000/8000/25,000/60,000/200,000. The chance that even a single voxel would reach this level of significance using the Bonferroni correction for multiple comparisons is $p < 0.002/0.006$ for 3/2 mm voxels.

corresponding p-value were used to identify voxels for which the counts were significantly different¹⁵. This indicates differential activation of that tissue volume, just as the differences found in functional MR images (fMRI) are interpreted as differential activation. Here the activation is neuroelectric whereas for fMRI, the activation represents tissue oxygenation. Hence this functional brain imaging method is named NeuroElectric Tomography (NET).

The results of these source counts for the whole brain are shown as a function of voxel size in Figure 4. Note that there is a consistent sharp increase in the number of voxels showing significant differential activation with voxel sizes of 6 and 4 mm with flattening

¹⁵ The χ^2 statistic of 32.8 with corresponding p-value = 3×10^{-8} were used as the threshold for significance. The corresponding joint p-value (Bonferroni correction) for finding at least 1 of the 200,000/60,000 $2\text{mm}^3/3\text{mm}^3$ voxels with $p < 3 \times 10^{-8}$ is 0.002/0.006.

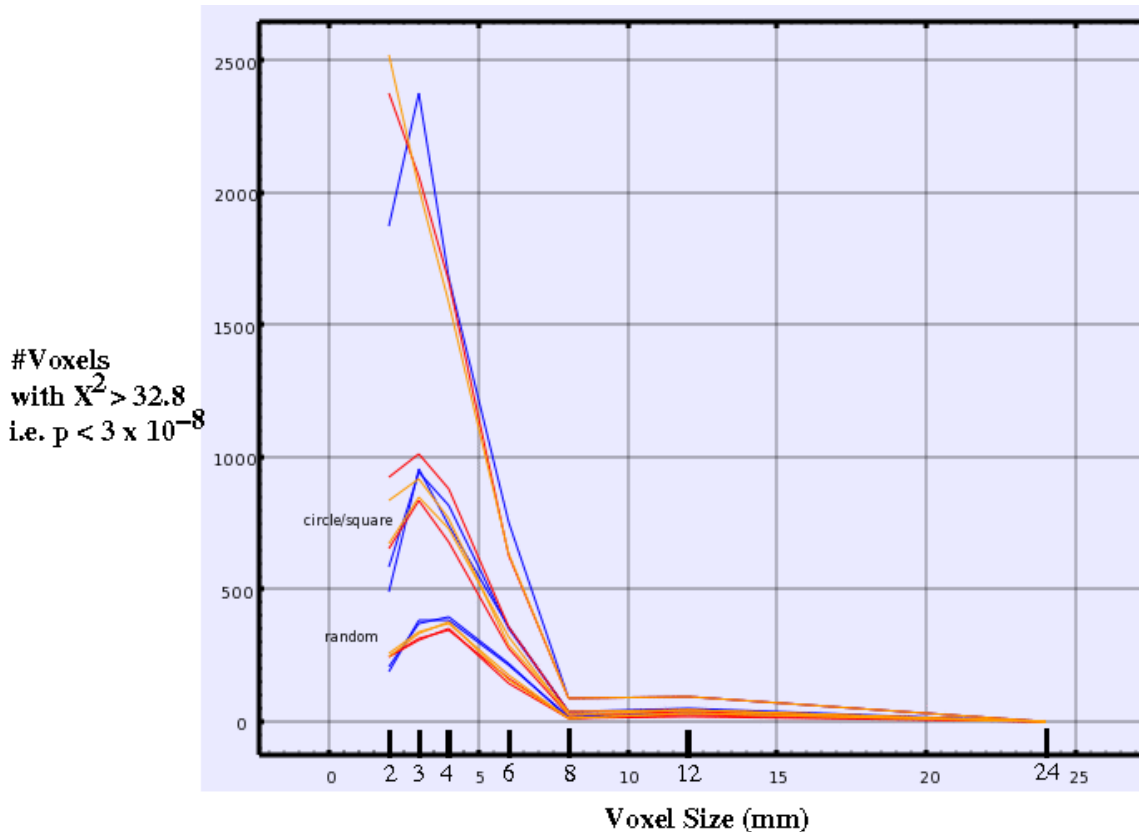


Figure 5. Repeat reliability for differential activation results is shown for 3 volunteers as in Figure 4. These are typical. For the 3 trace pairs marked: “random,” each source was randomly assigned to one of the 2 counts. For the 3 pairs marked: “circle/square,” the sources were assigned depending on the shape of the test figure. The “random” counts strongly demonstrate repeat reliability. Note the marked differences between the random counts and those sorted by shape, i.e. (1) decrease in the number of voxels with significant count differences for random assignment and (2) greater repeat reliability for random assignment. Here is additional strong evidence for the presence of task-related information in these source measures. Comparable results were found for sorting by green/blue and above/below.

or downturn of the curve at 3 mm. Since we are using a fixed threshold for the χ^2 statistic¹⁶, the power to reach that threshold decreases linearly as the total number of sources within each voxel decreases, i.e. as the size of the voxels decreases. Changing equally but opposite to this trend, the number of voxels increases with decreasing voxel size. The sharp change in slope of the curves at 6 mm shows that this is near the upper limit for the size of a functional unit.

¹⁶ $\chi^2 = \sum_{match, mismatch} (Observed - Expected)^2 / Expected$. The counts for sources found over the full set of ≈ 3000 voxels were used to compute the expected values.

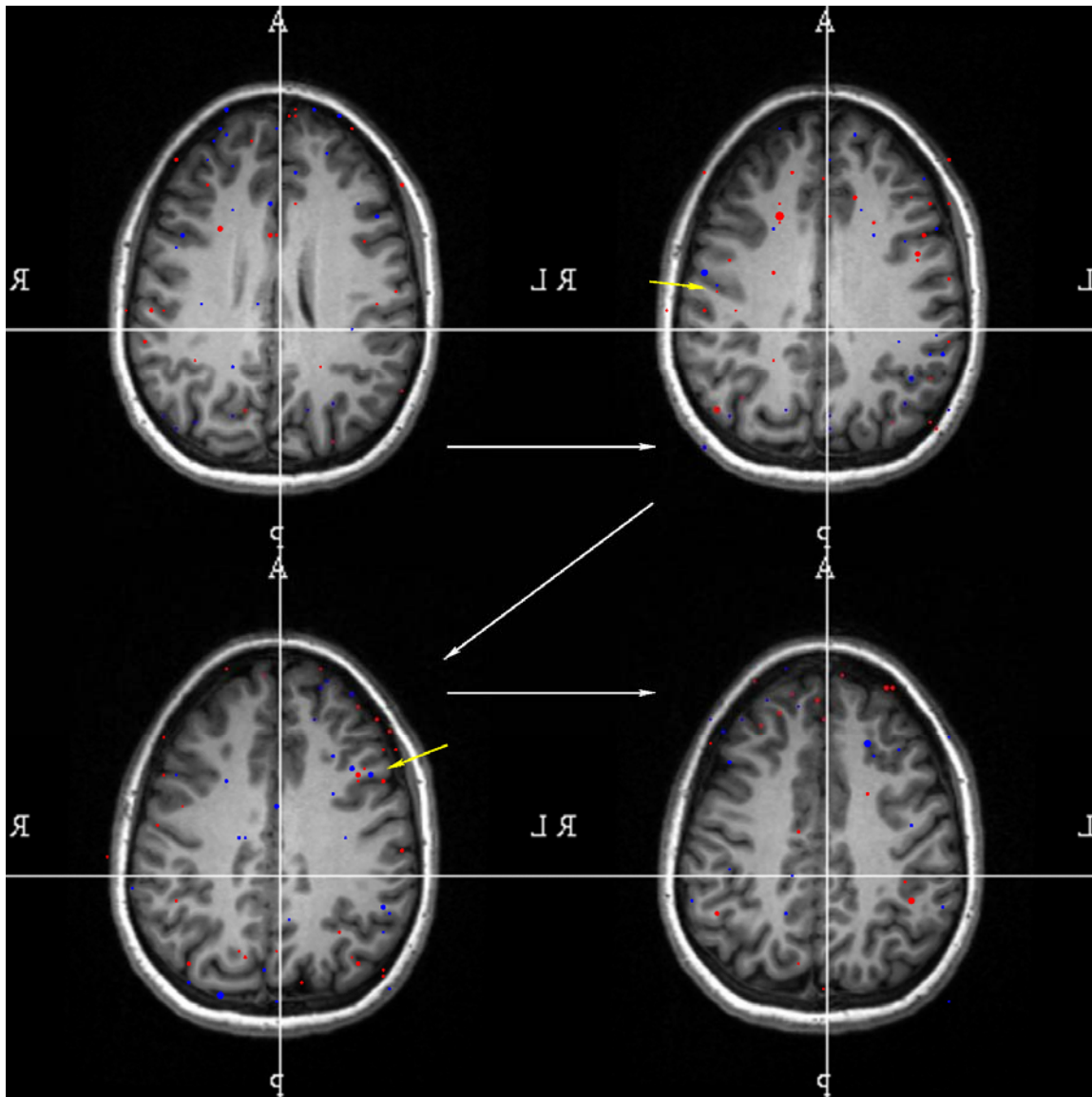


Figure 6. NeuroElectric Tomography (NET) – 4 of 41 3mm cuts are shown. The white arrows indicate progressively more superior cuts. The blue/red dots indicate voxels which are more highly activated ($p < 3 \times 10^{-8}$) during match/mismatch trials. The yellow arrows highlight adjacent voxels (3-4 mm apart) with opposite differential activation.

For these data, 3mm^3 voxels contain an average of ≈ 100 sources and a maximum of ≈ 500 . The average drops to ≈ 30 for 2mm^3 voxels; such low numbers produce a ceiling effect which readily accounts for the flattening/downturn of the curves for the smaller voxel sizes. This ceiling effect is more prominent in the repeat reliability results obtained with half counts (Figure 5). Yet at 3mm^3 with consequent reduced statistical power more than 400 voxels were found exceeding the threshold for differential activation. For 3mm^3 voxels the joint chance of finding 400 voxels which exceed the $\chi^2=32.8$ threshold is astronomical: 0.002^{400} . These results (1) provide evidence that 6 mm is a soft upper limit for the scale of functional units and (2) support the evidence of the correlation results (Figure 2) that MVR can resolve sources 2 mm apart.

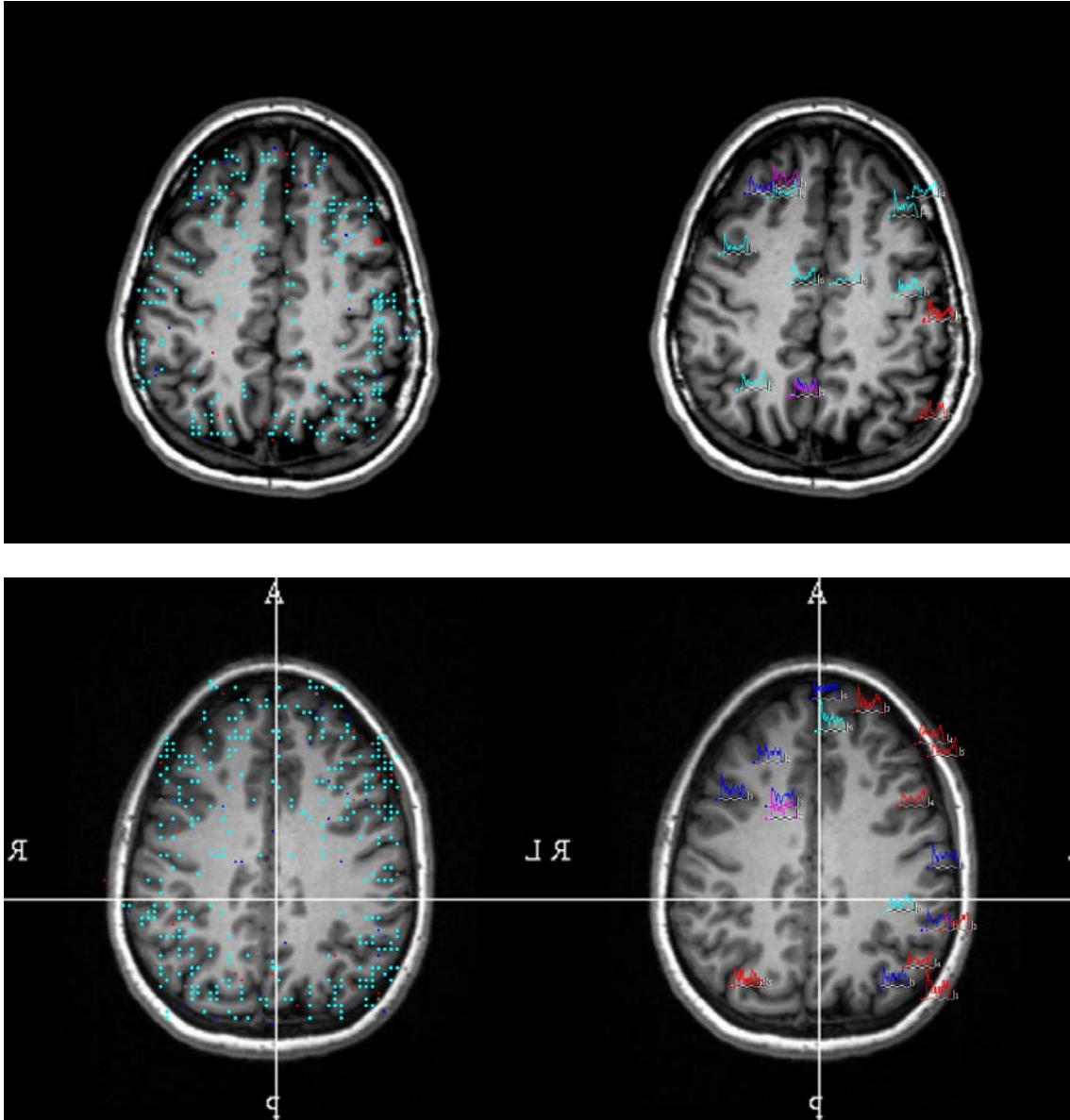


Figure 7: Preliminary examples (upper/lower from 2 volunteers) of dynamic information present in MVRs. **Left, differential sensitivity:** Voxels are highlighted (aqua) for which the number of sources was much greater than expected ($p < 3 \times 10^{-8}$). **Right, averaged MVR's** are shown for voxels which (1) showed differential sensitivity and (2) for which the averaged MVR under one condition was much more highly correlated to the grand average than the average for the complementary condition. Conditions: figure was (1) match(blue)/mismatch(red) to the sentence or (2) above(aqua)/below(magenta) the fixation point (Figure 2). Amplitude scale is indicated in nanoampere-meter units. Time scale is 500 msec.

A new kind of functional brain imaging. The voxels for which differential neuroelectric activation is found may be shown superimposed on MRI cuts to produce a neuroelectric tomogram (NET) (Figure 6). Note the adjacent voxels with opposite

activation highlighted with the yellow arrows in the figure. These results further support: (1) the resolving power of MVR is 2 mm or less and (2) the distance scale over which neural populations cooperate to produce functional units is ≈ 3 mm.

NET is 3-dimensional imaging of differentially activated tissue volumes comparable to that produced by functional magnetic resonance imaging, fMRI. Here are several points of comparison between the two functional imaging modalities.

1. For fMRI the underlying measure is tissue oxygenation. For NET the underlying measure is electrical current. They provide different information.
2. For fMRI, aggregated pixels are used to handle the multiple comparison problem so the voxel size is typically 6-10 mm. For NET no such aggregation is needed allowing a voxel size of 2 mm.
3. For fMRI, the differential activation occurs a minimum of 3 sec following the stimulus. For NET the differential activation spans the period 0-640 msec following the stimulus, a period which almost certainly can be substantially narrowed.
4. For fMRI, the end point of the primary data processing is the localization of differential activation. For NET, the individual waveforms found within each voxel may be further utilized to study both the neural dynamics within the tissue and the network of interactions between voxels. For these data, there were 50-500 waveforms found within each voxel. Connections between voxels can be visualized using High Definition Fiber Tracking (Verstynen, 2011) and functionally confirmed by network analysis using the localized virtual recordings provided by MVR.

fMRI is the leading functional brain imaging method and we have found a complementary approach which has considerably higher resolution and will almost certainly provide different information about brain function. Our hope is to find information in these scans which will enable differentiating between normal and concussion and will help us understand the pathophysiologic locus and mechanisms in concussion.

As noted in comparison 4. above, MVRs may be used to study both neural population and network dynamics. Figure 7 is a preliminary illustration of a small fraction of the dynamic information present in the MVRs. The differential sensitivity maps (left) are included (1) to detail the reduction process which was used to select the displayed waveforms (right) and (2) to show the marked respect shown to gray/white boundaries by the voxel selection. Although imperfect, the relative segmentation of the image due solely to identification of differential neuroelectric sensitivity is remarkable. While we do expect that populations of neural cell bodies with associated dendritic domains (gray matter) would be the primary sources of detectable magnetic fields, it is also reasonable to find some sources in white matter. These latter presumably represent populations of fibers through which synchronous volleys of action potentials pass. This presumption will be tested using the network analysis mentioned in comparison 4 above.

References

Anderson, E. Bai, Z. Bischof, C. Blackford, S. Demmel, J. Dongarra, J. Du Croz, J. Greenbaum, A. Hammarling, S. McKenney, A. Sorensen, D. LAPACK Users' Guide, Third Edition, Society for Industrial and Applied Mathematics, 1999, Philadelphia, PA.

Arciniegas DB. Clinical electrophysiologic assessments and mild traumatic brain injury: state-of-the-science and implications for clinical practice. *Int J Psychophysiol* 2011 Oct;82(1):41-52. <http://dx.doi.org/10.1016/j.ijpsycho.2011.03.004>

Bingham NH and JM Fry. *Regression: Linear Models in Statistics*. Springer, 2010.

Choe MC, Babikian T, DiFiori J, Hovda DA, Giza CC. A pediatric perspective on concussion pathophysiology. *Curr Opin Pediatr*. 2012 Dec;24(6):689-95. <http://dx.doi.org/10.1097/MOP.0b013e32835a1a44>

Davis GA, Iverson GL, Guskiewicz KM, Ptito A, Johnston KM. Contributions of neuroimaging, balance testing, electrophysiology and blood markers to the assessment of sport-related concussion. *Br J Sports Med*. 2009 May; 43 Suppl 1:i36-45. <http://dx.doi.org/10.1136/bjism.2009.058123>

Deutsch, M., R. Willis. *Software Quality Engineering: A Total Technical and Management Approach*. Englewood Cliffs, NJ: Prentice-Hall, 1988.

Dziemianowicz MS, Kirschen MP, Pukenas BA, Laudano E, Balcer LJ, Galetta SL. Sports-related concussion testing. *Curr Neurol Neurosci Rep*. 2012 Oct;12(5):547-59. <http://dx.doi.org/10.1007/s11910-012-0299-y>

Ellemberg D, Henry LC, Macciocchi SN, Guskiewicz KM, Broglio SP. Advances in sport concussion assessment: from behavioral to brain imaging measures. *J Neurotrauma*. 2009 Dec;26(12):2365-82. <http://dx.doi.org/10.1089/neu.2009.0906>

Fox WC, Park MS, Belverud S, Klugh A, Rivet D, Tomlin JM. Contemporary imaging of mild TBI: the journey toward diffusion tensor imaging to assess neuronal damage. *Neurol Res*. 2013 Apr;35(3):223-32. <http://dx.doi.org/10.1179/1743132813Y.0000000162>

Freeman, W and V DiPrisco, "Relation of olfactory EEG to behavior: time series analysis," *Behavioral Neuroscience*, 100(5): 753-763, 1986.

Gardner A, Kay-Lambkin F, Stanwell P, Donnelly J, Williams WH, Hiles A, Schofield P, Levi C, Jones DK. A systematic review of diffusion tensor imaging findings in sports-related concussion. *J Neurotrauma*. 2012 Nov 1;29(16):2521-38. <http://dx.doi.org/10.1089/neu.2012.2628>

Gonzalez PG, Walker MT. Imaging modalities in mild traumatic brain injury and sports concussion. *PM R*. 2011 Oct;3(10 Suppl 2):S413-24.

<http://dx.doi.org/10.1016/j.pmrj.2011.08.536>

Gosselin N, Saluja RS, Chen JK, Bottari C, Johnston K, Ptito A. Brain functions after sports-related concussion: insights from event-related potentials and functional MRI.

Phys Sports med. 2010 Oct;38(3):27-37. <http://dx.doi.org/10.3810/psm.2010.10.1805>

Hamalainen M and R. Ilmoniemi, "Interpreting magnetic fields of the brain: minimum norm estimates," *Med Biol Eng Comput*, Vol. 32, 35-42, 1994.

Hamalainen M, "The MNE Software," (visited 11Jul 2012):

http://www.nmr.mgh.harvard.edu/martinos/userInfo/data/MNE_register/index.php

Keightley ML, Chen JK, Ptito A. Examining the neural impact of pediatric concussion: a scoping review of multimodal and integrative approaches using functional and structural MRI techniques. *Curr Opin Pediatr*. 2012 Dec;24(6):709-16.

<http://dx.doi.org/10.1097/MOP.0b013e3283599a55>

Krieger D, T Berger, S Levitan, RJ Sciabassi, "An interactive toolset for characterizing complex neural systems", *International Journal of Computers and Mathematics with Applications* (20)4-6: 231 - 246, 1990.

Krieger D, "Spatio-temporal cortical patterns evoked in man by a discrimination task", *International Journal of Computers and Mathematics with Applications* 21(8): 29-52, 1995{1}

Krieger D, "A testable model of global cortical organization," *Int'l J. Neuroscience*, 83: 111-121, 1995{2}.

Kutcher JS, McCrory P, Davis G, Ptito A, Meeuwisse WH, Broglio SP. What evidence exists for new strategies or technologies in the diagnosis of sports concussion and assessment of recovery? *Br J Sports Med*. 2013 Apr;47(5):299-303.

<http://dx.doi.org/10.1136/bjsports-2013-092257>

Lin AP, Liao HJ, Merugumala SK, Prabhu SP, Meehan WP 3rd, Ross BD. Metabolic imaging of mild traumatic brain injury. *Brain Imaging Behav*. 2012 Jun;6(2):208-23.

<http://dx.doi.org/10.1007/s11682-012-9181-4>

McCullough BJ, Jarvik JG. Diagnosis of concussion: the role of imaging now and in the future. *Phys Med Rehabil Clin N Am*. 2011 Nov;22(4):635-52, viii.

<http://dx.doi.org/10.1016/j.pmr.2011.08.005>

McDonald BC, Saykin AJ, McAllister TW. Functional MRI of mild traumatic brain injury (mTBI): progress and perspectives from the first decade of studies. *Brain Imaging Behav*. 2012 Jun;6(2):193-207. <http://dx.doi.org/10.1007/s11682-012-9173-4>

Prabhu SP. The role of neuroimaging in sport-related concussion. *Clin Sports Med*. 2011 Jan;30(1):103-14, ix. <http://dx.doi.org/10.1016/j.csm.2010.09.003>

Rosenbaum SB, Lipton ML. Embracing chaos: the scope and importance of clinical and pathological heterogeneity in mTBI. *Brain Imaging Behav*. 2012 Jun;6(2):255-82. <http://dx.doi.org/10.1007/s11682-012-9162-7>

Sarvas J. 1987. Basic mathematical and electromagnetic concepts of the biomagnetic inverse problem. *Phys Med Biol* 32(1): 11-22.

Shenton ME, Hamoda HM, Schneiderman JS, Bouix S, Pasternak O, Rathi Y, Vu MA, Purohit MP, Helmer K, Koerte I, Lin AP, Westin CF, Kikinis R, Kubicki M, Stern RA, Zafonte R. A review of magnetic resonance imaging and diffusion tensor imaging findings in mild traumatic brain injury. *Brain Imaging Behav*. 2012 Jun;6(2):137-92. <http://dx.doi.org/10.1007/s11682-012-9156-5>

Slobounov S, Gay M, Johnson B, Zhang K. Concussion in athletics: ongoing clinical and brain imaging research controversies. *Brain Imaging Behav*. 2012 Jun;6(2):224-43. <http://dx.doi.org/10.1007/s11682-012-9167-2>

Tormenti M, D Krieger, A Puccio, M McNeil, W Schneider, DO. Okonkwo. Magnetoencephalographic virtual recording: a novel diagnostic tool for concussion. *J. Neurosurgery*, accepted for publication, 2012.

Verstynen T, Jarbo K, Pathak S, Schneider W. In vivo mapping of microstructural somatotopies in the human corticospinal pathways. *J Neurophysiol*. 2011 Jan; 105(1):336-46.

Grants

DSF Charitable Foundation, 2013-2016. Pittsburgh High Definition Fiber Tracking (HDFT) Traumatic Brain Injury (TBI) Transformative Advancement Plan. PI: Walter Schneider.

Department of Defense #13154004, 2014-2016. Targeted evaluation, action, and monitoring of traumatic brain injury (TEAM-TBI). PI: David O. Okonkwo.